# Continuous-membrane surface-micromachined silicon deformable mirror

**Thomas G. Bifano**
**Raji Krishnamoorthy Mali,** MEMBER SPIE
**John Kyle Dorton**
**Julie Perreault**
**Nelsimar Vandelli**
**Mark N. Horenstein**
**David A. Castañon**
Boston University
College of Engineering
Boston, Massachusetts 02215
E-mail: tgb@bu.edu

**Abstract.** The authors describe the development of a new type of micromachined device designed for use in correcting optical aberrations. A nine-element continuous deformable mirror was fabricated using surface micromachining. The electromechanical behavior of the deformable mirror was measured. A finite-difference model for predicting the mirror deflections was developed. In addition, novel fabrication techniques were developed to permit the production of nearly planar mirror surfaces.
© *1997 Society of Photo-Optical Instrumentation Engineers.* [S0091-3286(97)00405-4]

Subject terms: micro-opto-electro-mechanical systems; deformable mirror; surface-micromachined; adaptive optics.

Paper MEM-04 received Oct. 6, 1996; revised manuscript received Jan. 10, 1997; accepted for publication Jan. 17, 1997.

## 1 Introduction

One of the successful optical applications of surface micromachining has been the development of electrostatically actuated micromechanical mirror arrays—massively parallel arrays of coordinated, movable reflective or refractive elements—for use in projection display systems.[1] Each element is a mirror segment that serves as a pixel in a larger display, and the actuation of elements is coordinated in parallel, using binary digital control signals. In such systems, it has been demonstrated that the fabrication yield of simple micromechanical actuators can approach 100%. Further, it has been established that large-scale integration of electronics with micro-electro-mechanical system (MEMS) array structures is achievable. This integration has been performed by building the MEMS structures on top of a planarized CMOS electronics array.

Several extensions of these basic concepts have been proposed to enable the development of a surface-micromachined continuous-membrane deformable mirror for use in adaptive optics systems. In adaptive optics, it is important that the deformable mirror be both continuous and precisely adjustable. The devices described in this paper are the first continuous mirrors to be made using surface micromachining techniques. (Bulk-micromachined continuous mirrors have been previously demonstrated.[2]) The surface-micromachined mirrors have been designed, fabricated, and tested at Boston University. The device consists of a single compliant optical membrane supported by multiple attachments to an underlying array of surface-normal electrostatic actuators.

Two features distinguish this device from previous surface-micromachined mirror systems. First, the mirror surface is continuous instead of being segmented. As a result, local deformation by an actuator causes a smooth deflection of the mirror surface, with no discontinuities in the surface contour, no diffractive interference due to segment edges, and no loss of optical intensity due to fill factors lower than unity. Also, the new deformable mirror device allows precise, continuous control of the mirror membrane's local deflection in the surface-normal direction. This means the electrostatic control signals are continuously variable and provide nanometer-scale precision in positioning the mirror membrane at each of its attachment points.

The primary variables to be specified in a deformable mirror system are the number of actuators, the control bandwidth, the maximum actuator stroke, and the resolution. The design goals for the MEMS continuous mirror are based on the requirements of a typical adaptive optical imaging system. Such a system can be used for astronomical observations, whose design parameters can be estimated from the desired strehl ratio (which is the ratio of the on-axis intensity of an aberrated image to that of an unaberrated image), the optical wavelength of interest, the characteristics of the optical disturbance, and the optical-system aperture, using theoretical turbulence and photonic models.[3,4] For example, based on assumptions of moderate turbulence, near-infrared light ($\lambda = 1.0\ \mu$m), a 1-m-diam primary mirror, and a strehl ratio of 0.2, a deformable mirror would require 400 actuators, an open-loop bandwidth of 1 kHz, a stroke of 2 $\mu$m, and a position resolution of 20 nm.[5]

## 2 Fabrication

A surface micromachining process uses alternating layers of structural material (often polycrystalline silicon) and sacrificial material (often silicon dioxide). For the devices described in this paper, the foundry Multi-User MEMS Process (MUMPs) at the Microelectronics Center of North Carolina was used for processing (see Fig. 1). This is a three-layer polycrystalline silicon (polysilicon) surface-micromachining process. A base nitride layer insulates the surface micromachined layers from the underlying silicon wafer. The first polysilicon layer is used to create an array of electrode pads for the electrostatic actuators. It is also used for routing polysilicon wires on the substrate surface. The first silicon dioxide (oxide) layer defines the space that eventually becomes the air gap for the parallel-plate

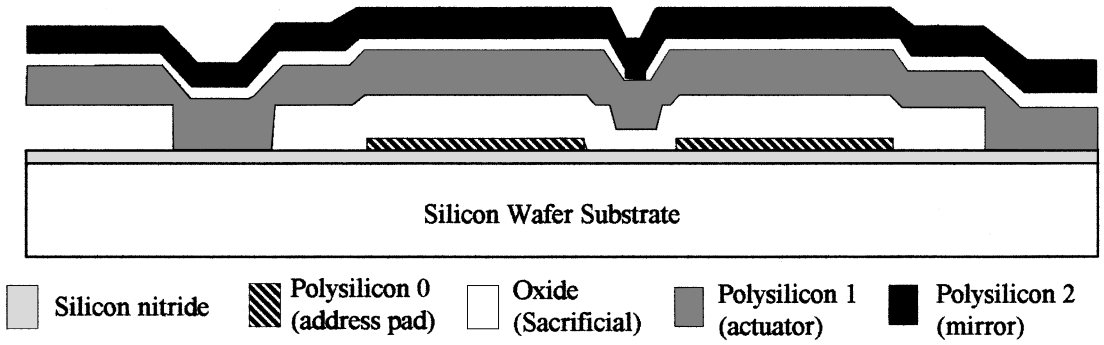


**Fig. 1** Schematic of fabricated-deformable-mirror test structure using MUMPs.

surface-normal electrostatic actuators. On top of the first oxide, the first polysilicon layer is deposited and patterned into an array of fixed-end double cantilevers that act as the second electrodes for each of the electrostatic actuators. The second oxide layer creates a gap between the electrostatic actuators and the second polysilicon layer, which serves as the mirror membrane. Anchor holes in the second oxide allow attachment of this polysilicon mirror to the center of each cantilever electrostatic actuator. A voltage imposed across the actuator's opposing electrodes results in electrostatic attraction, which causes the cantilever to deflect toward the substrate.

The principal attributes required of the as-fabricated deformable mirror are that it be planar and that it be continuous. Early versions of the device described in this paper exhibited excessive nonplanarity on the mirror surface, due to the conformal growth processes inherent in surface micromachining. Typically, in surface micromachining, each patterned layer adds contour variations approximately equal to its own thickness to subsequent layers. For the MCNC MUMPs process, for example, contour variations (e.g., nonplanarity) on the mirror surface generally add up to about 5 $\mu$m. Since the mirror itself has a thickness of less than 2 $\mu$m, postfabrication planarization through polishing or lapping is not possible.

Based on a design strategy developed in collaboration with MCNC, acceptably planar surfaces were obtained when all cuts in polysilicon and oxide layers were restricted to widths no larger than 1.5 $\mu$m. With pattern sizes restricted to this width, the conformal deposition processes in micromachining act to rapidly fill in cuts from previously deposited layers, largely attenuating the magnitude of their ''print-through'' to subsequent layers. As a result, greater planarity in the uppermost layers is achievable. Anchoring sites, which would be structurally weak if only 1.5 $\mu$m in width, are fabricated as honeycombs of thin polysilicon walls encapsulating a thicker structure of oxide. Figure 2 is a schematic illustrating this design concept.

The success of this processing strategy for planarization is illustrated in Figure 3. The top SEM photo is of a MEMS mirror supported on 16 cantilever actuators, fabricated using the MUMPs process without efforts toward planarization. The underlying features (electrostatic actuators and polysilicon electrodes) emboss the mirror membrane, leading to poor planarity. At the bottom is a MEMS mirror supported over a nine-element array of actuators. In the planarized mirror, no ''print-through'' of underlying structures is observed. Qualitative examination using scanning electron microscopy indicates significant gains in surface planarity achieved though this technique. Detailed quantitative measurements of surface contour are planned in the near future.

## 3 Actuator Design and Characterization

The heart of the actuation system for these devices is an array of double-cantilever electrostatic actuators, one of which is shown in Fig. 4.

The critical issues relating to device performance are yield (indicating process reliability), position repeatability, and frequency response. In a systematic evaluation of these parameters reported previously,[6] hundreds of individual actuators were tested. The results were promising: Fabrication through MCNC MUMPs yielded 94.5% useful, working actuators. Electromechanical performance was evaluated by driving the actuators with a high-speed voltage controller and measuring the dynamic motion response. It was found that actuators exhibited no hysteresis and that they could be repeatedly positioned to a precision of 10 nm. Moreover, their frequency response was measured to be at least 66 kHz for the particular actuators tested.

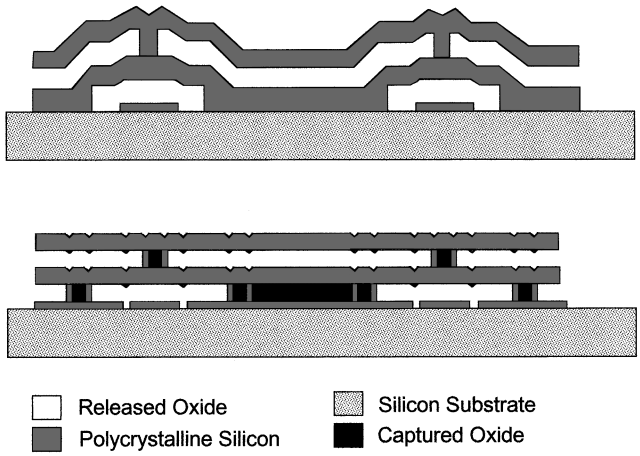


**Fig. 2** Top: cross section of conventional surface-micromachined structure, illustrating nonplanarity. Bottom: cross section of new design for continuous deformable mirror to achieve planar mirror surface.

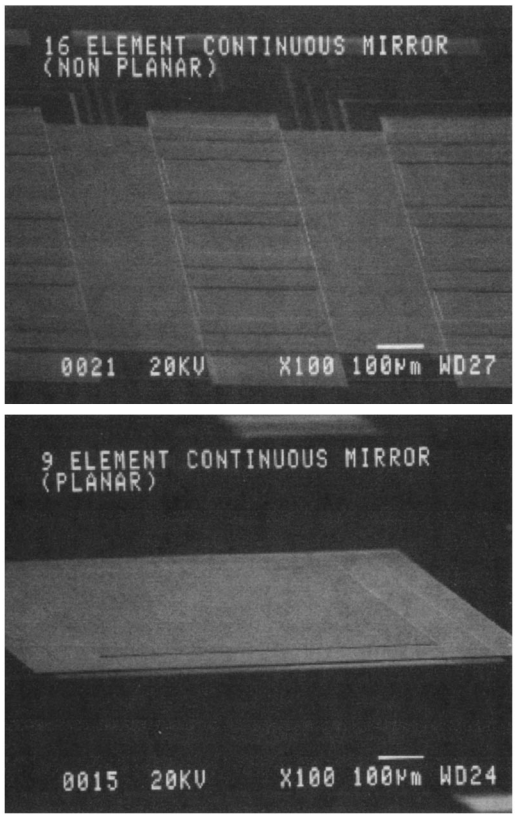


**Fig. 3** Planarization results for surface-micromachined mirrors.

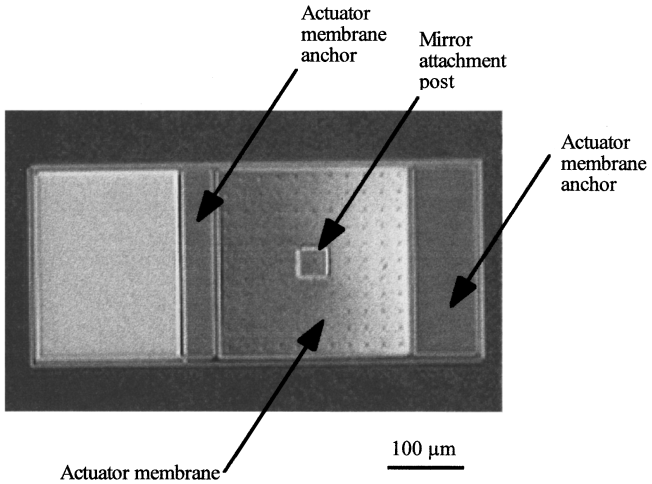


**Fig. 4** Microphotograph of an individual test actuator (no mirror membrane attached).

## 4 Development of a Nine-Element Planar Mirror Prototype

A nine-element continuous mirror prototype was fabricated through the MUMPs foundry process. Table 1 lists the dimensional specifications of the mirror prototype. Figure 5 shows a schematic representation of the nine-element mirror, with the fixed-fixed actuators on a silicon substrate and a mirror membrane attached to the actuators by posts. At the bottom is a microphotograph of the fabricated device.

**Table 1** Dimensions of test mirror.

| | |
|---|---|
| Number of actuators | 9 |
| Mirror dimensions | $560\times560\times1.5$ $\mu$m |
| Actuator cantilever dimensions | $200\times200\times2.0$ $\mu$m |
| Actuator gap | 2.0 $\mu$m |
| Interactuator spacing | 250 $\mu$m |

Deflections were measured using the Zygo ZMI 1000 system—a single-point, split-frequency, displacement-measuring laser interferometer. This device uses a focused laser beam to measure normal displacement with a position resolution of 2.5 nm, a range of $\pm250$ $\mu$m, a frequency bandwidth of 0 to 133 kHz, and a lateral averaging area of several micrometers. The incoming laser beam has two components that are orthogonally polarized and 20 MHz apart in frequency. This beam is divided by the polarization beamsplitter into the two orthogonally polarized components (Fig. 6). The reference beam passes through the quarterwave plate and is reflected back from the retroreflector. The measurement beam passes through a quarterwave plate and is focused on the measurement surface. Displacement of the measurement surface causes a change in the optical path difference of the two beams. The interference of the recombined beams is converted into a 16-bit binary representation of displacement.

An important performance criterion for the deformable mirror is a predictable and repeatable influence function. The influence function is defined as the surface-normal displacement field on the mirror due to displacement of a single actuator attachment post. Influence functions were experimentally measured for the center, a side, and a corner actuator (actuators 5, 4, and 1, respectively, in Fig. 5). Fig-

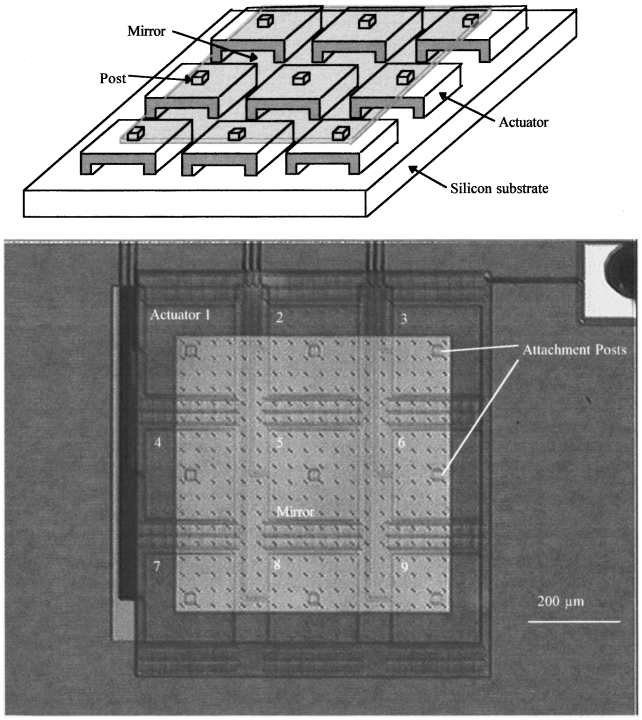


**Fig. 5** Schematic of nine-element mirror (top) and optical micrograph of nine-element, planarized continuous mirror (bottom).

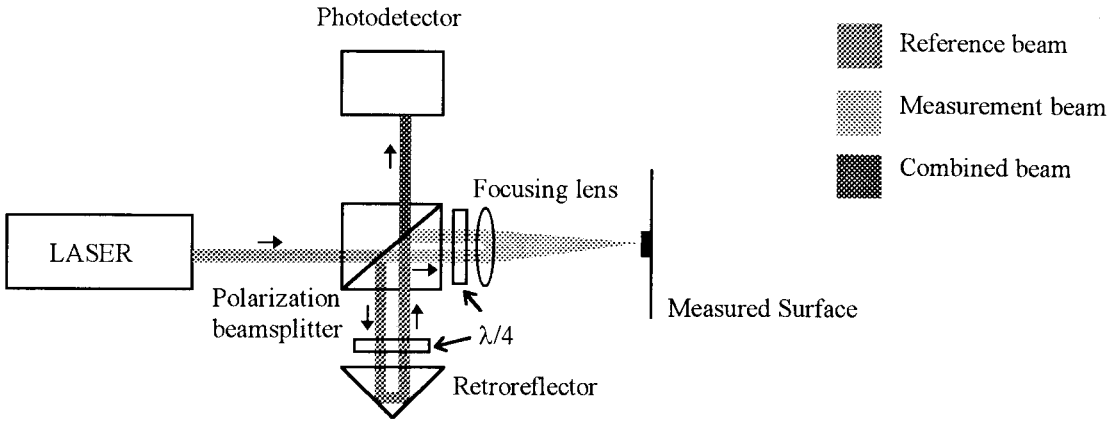


**Fig. 6** Laser interferometer system used for device characterization. Motion resolution is 2.5 nm, and measurement bandwidth is 133 kHz.

ures 7, 8, and 9 show the measured mirror surface and projected contour plot for each case. The displacement at the center of the mirror due to an increasing voltage on the central actuator is shown in Fig. 10.

## 5 Numerical Modeling of Prototype Mirror

We developed a numerical algorithm to model the behavior of the continuous mirror deflected by an electrostatically activated microactuator. The critical modeling issues, concerning boundary conditions and deflection compatibilities between the actuator and the mirror, are presented here.

The method of finite differences as applied to plate theory was used to numerically simulate the mechanics of the electrostatic actuator and of the continuous deformable mirror. The general partial differential equation for plate bending is

$$\nabla \cdot \nabla w(x,y) = \frac{q}{D}, \tag{1}$$

where $w$ is the deflection of the plate, $q$ the distributed loading, and $D$ the flexural rigidity of the plate. The continuous problem was discretized into equally spaced arrays for the actuators and the continuous mirror as shown in Fig. 11. The finite-difference equivalent for this equation[7] was then applied to the arrays. The boundary conditions for the actuators consisted of two clamped and two free edges. The clamped-edge boundary conditions are obtained by applying the zero-slope condition at the edges. The boundary conditions on the membrane mirror required that all edges be free. The free-edge boundaries yield two new differential equations,

$$\frac{\partial^2 w}{\partial x^2} + \upsilon \frac{\partial^2 w}{\partial y^2} = 0, \quad \frac{\partial^3 w}{\partial x^3} + (2-\upsilon) \frac{\partial^3 w}{\partial x\, \partial y^2} = 0, \tag{2}$$

which represent zero moment and zero shear on the free edge when the edge is normal to the $x$ axis. These equations are solved simultaneously with the homogeneous plate bending equation to obtain the simulated deflections.

The loading conditions on the electrostatically activated actuator were determined using a deflection-dependent load formula,

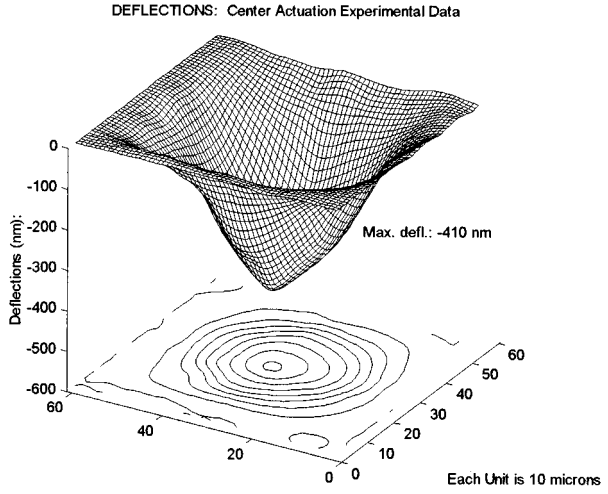


**Fig. 7** Surface profile and contour map of the measured influence function of the center actuator.

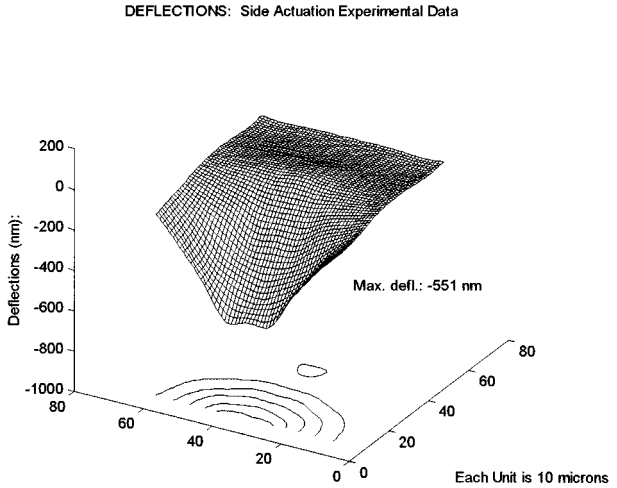


**Fig. 8** Surface profile and contour map of the measured influence function of the edge actuator.

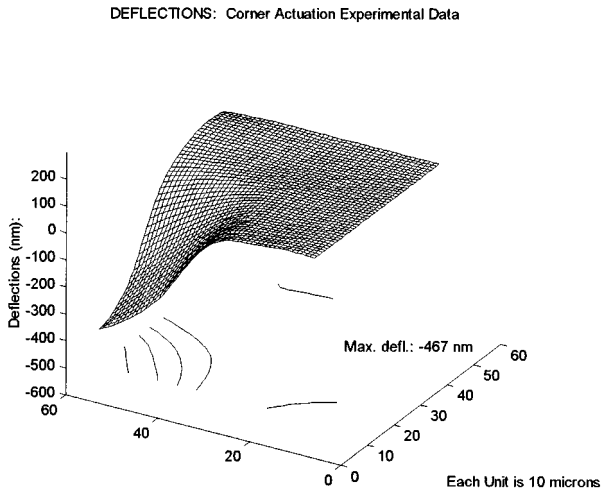


**Fig. 9** Surface profile and contour map of the measured influence function of the corner actuator.

$$q_{i,j}=\frac{k^2\epsilon V^2}{2(g-y_{i,j})^2}, \tag{3}$$

where $k$ is the dielectric constant for air, $\epsilon$ is the permittivity of free space, $V$ is the voltage, $g$ is the gap between the actuator and the electrostatic pad, $y$ is the deflection, and $i,j$ are the discretized locations in the $x,y$ domain of the actuator array. Since the loading on the actuator varies as the inverse square of the deflection, extreme loading conditions (high voltage on the actuator) result in solutions that converge to deflections that are beyond geometrically constrained limits. These solutions represent loading conditions that are beyond a critical voltage for which the solutions cannot be obtained with the finite-difference method.

The loading condition on the mirror as a result of the electrostatic actuation was obtained by matching deflections of the mirror and the actuator at the location where the two are attached by a post. An iterative process was used to find the correct load that resulted in matched deflections for each actuator in the 3-by-3 array.

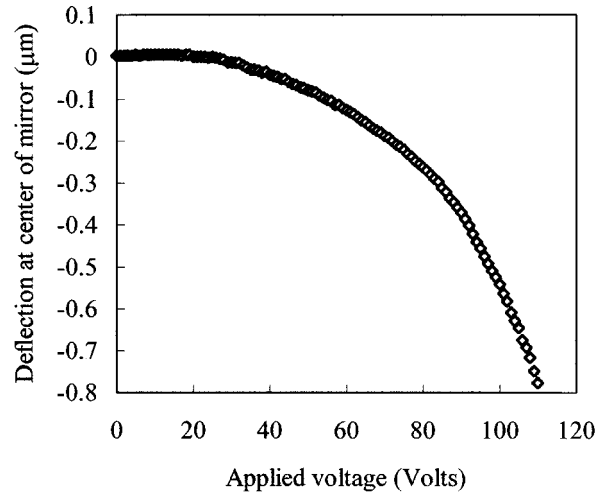


**Fig. 10** Static response of mirror center for an active central actuator.

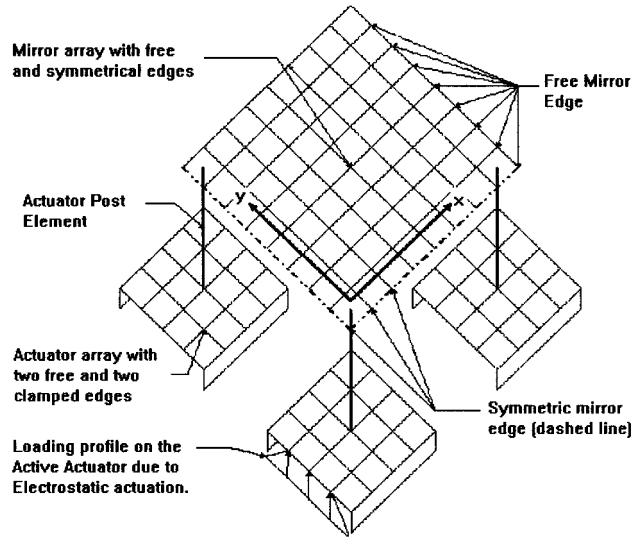


**Fig. 11** Schematic for numerical model of mirror using finite differences.

### 5.1 *Simulation Results*

A relaxation method was used to minimize the finite-difference residuals during iteration. Preliminary results showed that denser discretization of the actuator and mirror arrays yielded more accurate deflections. Figure 12 shows simulated deflections of a mirror with free edges. These compare well with the measured deflections shown in Fig. 7 for a mirror subjected to the same conditions.

## 6 Discussion

The actuators exerted influence functions on the mirror that resulted in approximately 10% deflection at adjacent actuator locations. The magnitude of this influence is appropriate for adaptive optics applications. Larger influences would introduce excessive cross talk between adjacent actuators and further complicate the dynamic control of the mirror.

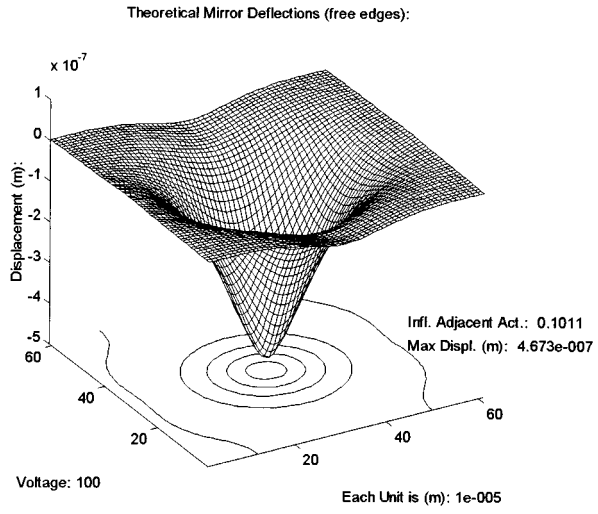


**Fig. 12** Theoretical deflections for a continuous mirror with free edges over a 3-by-3 array of actuators with voltage applied to the center actuator.

On the other hand, small influences would limit the smoothness of the mirror surface, degrading optical performance.

The peak deflection obtained with this mirror was 0.8 $\mu$m. However, this stroke is a function of the gap, which was in turn was limited by the standardization imposed by the foundry fabrication process. Fabrication processes can be modified to attain higher strokes by increasing the gap size. Deformable mirrors with a 2-$\mu$m stroke mounted on a 400-element actuator array are currently being fabricated.

When subjected to 100 V at the center actuator, the measured deflection was 410 nm and the measured influence on adjacent actuators was in the range of 5% to 10%. The predicted deflection under the same conditions was 467.3 nm with an influence of 10.11%. The numerical estimates of the peak deflection and influence functions of the mirror thus compare well with experimental data. Based on this model, algorithms can be developed to predict mirror shapes when arbitrary voltages are applied to different actuators. Further, in a real-time actuation system, it will be necessary to predict the required voltages on the actuator array in order to generate a specific mirror shape corresponding to the aberration being compensated for.

## *Acknowledgments*

This research is being funded in part by a three-year contract with ARPA (DABT63-95-C-0065) at Boston University. The authors would like to thank MCNC for collaboration on the processing issues and Prof. Ray Nagem for his valuable contributions to the simulation effort.

## *References*

1. J. M. Younse, ''Mirrors on a chip,'' *IEEE Spectrum*, 27–31 (Nov. 1993).
2. G. Vdovin and L. Sarro, ''Flexible reflecting membranes micromachined in silicon,'' *Semiconductor Sci. and Technol.* **9**, 1570–1572 (1994).
3. J. E. Pearson and S. Hansen, ''Experimental studies of a deformable-mirror adaptive optical system,'' *J. Opt. Soc. Am.* **67**(3), 325–333 (1977).
4. R. J. Tyson, *Principles of Adaptive Optics*, Academic Press, San Diego (1990).
5. R. Krishnamoorthy, T. Bifano, and N. Vandelli, ''Development of MEMS deformable mirrors for phase modulation of light,'' Opt. Eng. **36**(2), 542–548 (1997).
6. R. Krishnamoorthy, T. Bifano, and G. Sandri, ''Statistical performance evaluation of electrostatic micro actuators for a deformable mirror,'' in *Microelectronic Structures and MEMS for Optical Processing II*, Austin TX, Oct. 14–15, 1996, *Proc. SPIE* **2881**, 35–44 (1996).
7. S. Timoshenko and S. Woinowsky-Krieger, *Theory of Plates and Shells*, 2nd ed., McGraw-Hill, NY (1959).

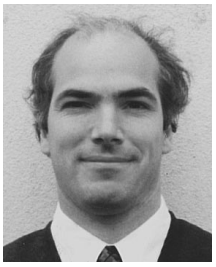

**Thomas G. Bifano** received BS and MS degrees in mechanical engineering and materials science from Duke University in 1980 and 1983, respectively, and a PhD in 1988 in mechanical engineering from North Carolina State University. Since joining the faculty of Boston University in 1988, he has developed an internationally known research program to study ultraprecision machining. He directs the Boston University Precision Engineering Research Laboratory, where he oversees currently active projects on ion machining of ceramics, ceramic hard-disk substrate fabrication, and silicon micromachining of deformable mirror systems.

**Raji Krishnamoorthy Mali** received a BS in mechanical engineering from the University of Bombay, India, in 1992. She was a Presidential University Graduate Fellow at Boston University and received an MS in mechanical engineering in 1994. She is currently a doctoral student at Boston University, and is involved in the development of a surface micromachined deformable mirror for adaptive optics applications.

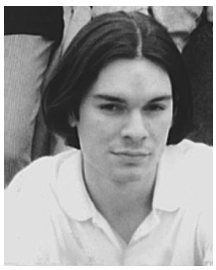

**John Kyle Dorton** received an MS in mechanical engineering from Boston University in 1996. His research included finite difference/finite element modeling of electromechanical systems. He is currently working for Sander Hansen A/S in Denmark.

**Julie Perreault** received a BS in electrical engineering from Boston University in August 1996. She worked as a design engineer at P&E Microcomputer Systems developing research and development tools for microprocessors. She is currently in the PhD program in electrical engineering at Boston University. She is interested in controls and is working on position sensing technology for micro-electro-mechanical structures.

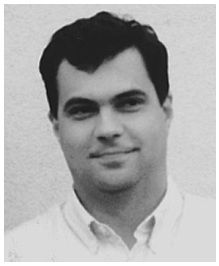

**Nelsimar Vandelli** received a BS in mechanical engineering from the Military Institute of Engineering, Brazil, in 1986. He worked at the Brazilian Petroleum Company from 1987 to 1991. He was accepted in the postbachelor PhD program in mechanical engineering at Boston University in September 1994. He taught mechanics of materials on an undergraduate level in the summers of 1994 and 1995. His current research includes the theoretical and numerical modeling of micro-electro-mechanical devices using finite element analysis. He is also interested in rarefied microflows in fluidic micro-opto-mechanical systems devices.

**Mark N. Horenstein** received his BS and PhD degrees in electrical engineering from the Massachusetts Institute of Technology in 1973 and 1978, respectively, and his MS degree in electrical engineering from the University of California in Berkeley in 1975. From 1978 to 1979, he was a research scientist and development engineer for Spire Corporation in Bedford Massachusetts. In 1979, he joined the faculty in the Department of Electrical and Computer Engineering at Boston University where he is now an Associate Professor. He specializes in the field of electrostatics and its application to problems in research and industry. He is the author of numerous papers on topics in electrostatics, including the development of electric field and ion measuring instrumentation, the use of air ions to neutralize moving webs and fabrics, the effects of electrostatic charge on the opening of parachutes, and the use of ions to detect defects in barrier membranes. He also holds several patents related to electrostatic devices and processes. He joined the Boston University micro-opto-mechanical systems team in 1995.

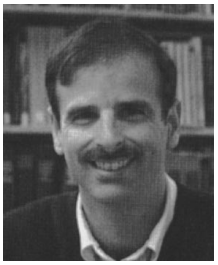

**David A. Castañon** has been active in systems engineering and control design for over 18 years. He received his BS in electrical engineering from Tulane University in 1971, and his PhD in applied mathematics from the Massachusetts Institute of Technology in 1976. He was Senior Scientist of ALPHATECH, Inc., a small engineering firm in Burlington, Massachusetts, until 1990, when he joined the Boston University Faculty. His research interests include signal and image processing, control, and estimation, with applications to multitarget tracking and command and control. He has more than 100 refereed journal and conference publications.